Fracture Mechanics of Concrete and Concrete Structures -
Recent Advances in Fracture Mechanics of Concrete - B. H. Oh, et al.(eds)

Discrete modeling of structural elements

A. DELAPLACE
LMT-Cachan, ENS de Cachan / CNRS UMR 8535 / Université Paris 6
A. TOGNEVI
LMT-Cachan, ENS de Cachan / CNRS UMR 8535 / Université Paris 6
CEA Saclay, DEN/DPC/SCCME/LECBA
B. BARY
CEA Saclay, DEN/DPC/SCCME/LECBA

ABSTRACT: This paper presents a discrete element model dedicated to model the behavior of reinforced concrete structures. Starting for a standard discrete model, a strategy is proposed to take into account the reinforcement bars into the material, while keeping the initial numerical efficiency and robustness of the discrete model: no degrees of freedom are added in the numerical problem and the efficient "elastic prediction algorithm" can still be applied when linear behavior is considered for the rebars. Rebars meshing is obtained by rearranging the location of the particle nuclei around the bars, and an additional model parameter is introduced for accounting the behavior of the steel-concrete interface. The capabilities of the proposed approach is illustrated by several comparisons with experimental results, either in 2D or 3D.

1 INTRODUCTION

Discrete element models have shown their ability to represent cracking in brittle heterogeneous materials (Cundall and Strack 1979; Kun and Herrmann 1996; Delaplace, Roux, and Pijaudier-Cabot 2001). In particular, they have been used to study the concrete behaviour (Schlangen and Garboczi 1997; Bolander and Saito 1998; Van Mier and Van Vliet 2003; Delaplace and Desmorat 2007): discrete models take into account the material heterogeneity, crack (see as a discontinuity in the model) is naturally represented, allowing the computation of its length, its aperture. Furthermore, they are robust in a numerical sense because the uniqueness of the solution is guaranteed. The main drawbacks of these models is the large number of elements that should be considered, leading to excessive computational times.

Needs for numerical simulation of reinforced concrete structures is always increasing with an even more refined description of the damage zone: recent engineers rules (see for example the EuroCodes 2 in Europe) are based on an explicit description of the crack pattern. The widely used finite element approach is then sometimes not sufficient to obtain this fine crack pattern, due to the macroscopic approach of such model. Then, the use of a discrete element model can be considered to obtain this fine crack pattern, under the condition that reinforcement bars are added in the model (note that for a too large structure leading to a prohibitive computational time, a coupled finite element/discrete element approach could be used (Chiaia, Vervuurt, and Van Mier 1997; Xiao and Belytschko 2004; Rojek and Onate 2007)). The goal of this study is to provide a numerical strategy to include rebars in a discrete model.

2 DISCRETE MODEL

A discrete particle model is used to represent the behavior of concrete, considered here as an isotropic brittle material. Cohesion forces link the initially neighbored particles, and a perfectly brittle behavior is assigned to each link. The force of such model is its simplicity that leads to a robust and efficient numerical implementation. The drawback is of course the number of particles that should be considered to obtain a pertinent discretization at the material mesoscale.

2.1 *Random mesh*

The particle assembly is computed from a Voronoi tessellation. A preliminary regular grid is mapped onto the geometry that the user wants to mesh (figure 1), and a nuclei cell is allocated randomly into each grid cell (Moukarzel and Herrmann 1992). This procedure allows an easy classification of the particles and an easy application of the boundary conditions.

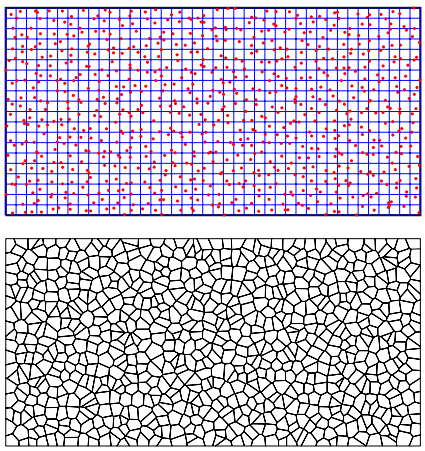

Figure 1. The initial regular grid plotted on the sample with one nucleus per case (top) and the final Voronoi tessellation (bottom).

2.2 *Cohesion forces*

Basically, a cohesion link between two particles is represented with a local $n_{\text{dof}} \times n_{\text{dof}}$-matrix, where n_{dof} if the number of degrees of freedom for each particles: $n_{\text{dof}} = 3$ in 2D (two translations and one rotation) and $n_{\text{dof}} = 6$ in 3D (three translations and three rotations). An Euler-Bernoulli beam matrix is used as the link matrix. Hence, four parameters should be identified for each links:

- the beam area A_b and the beam length ℓ_b, imposed by the mesh geometry (respectively the boundary size between the two particles and the distance between the cells nuclei),
- the beam Young modulus E_b, chosen to be identical for all beams,
- the inertia coefficient I_b (or the dimensionless parameter $\alpha = I_b/I_O$ where I_O is the inertia coefficient of an equivalent circular section).

The protocol to identify the two last parameters has been detail in (Woestyn, Delaplace, and Koechlin 2006) in 2D and in (Delaplace and Desmorat 2007) in 3D. In summary, the inertia coefficient I_b is first obtained by identifying the material Poisson coefficient, then E_b by identifying the Young modulus material (changing E_b does not affect the apparent material poisson coefficient). A key point is that the material elastic parameters is independent of the mesh discretization if a sufficient number of particles are taken into account: roughly 100 particles per unit length in 2D and 15 particles per unit length in 3D are the numbers to be considered for a pertinent discretization.

2.3 *Nonlinear behavior*

The material nonlinear behavior is obtained by considering a perfectly brittle law for the beams (Hermann and Roux 1990; Van Mier and Van Vliet 2003; D'Addetta 2004; Delaplace and Ibrahimbegovic 2006). A beam ij linking particles i and j breaks if the following condition is fulfilled:

$$P_{ij}\left(\frac{\varepsilon_{ij}}{\varepsilon_{ij}^{cr}}, \frac{|\theta_i - \theta_j|}{\theta_{ij}^{cr}}\right) \geq 1 \qquad (1)$$

where ε_{ij} is the beam strain, θ_i and θ_j are respectively the rotations of particle i and j. ε_{ij}^{cr} and θ_{ij}^{cr} are two model parameters identified by fitting respectively the tensile strength and the compressive strength of the material (Woestyn, Delaplace, and Koechlin 2006; Delaplace and Desmorat 2007; Delaplace 2009). This simple brittle law is sufficient to represent the main features of the concrete behavior: the decrease in material stiffness as the microcracks occur, the large dissymmetry in tension/compression behavior. A second asset of this brittle law is that an elastic prediction algorithm (presented next) can be used, ensuring the solution uniqueness.

2.4 *Numerical solver*

The solution of a problem using the previous discrete model is obtained by solving the general discrete equilibrium equation $\mathbf{K}(\mathbf{u})\mathbf{u} = \mathbf{f}$, where $\mathbf{K}$ is the global stiffness matrix, $\mathbf{u}$ the displacement vector and $\mathbf{f}$ the loading vector. One prefers to use the so-called elastic prediction algorithm, where just one beam is broken at each step (Chiaia, Vervuurt, and Van Mier 1997; Schlangen and Garboczi 1997; Rots, Invernizzi, and Belletti 2006; Delaplace and Desmorat 2007). For the loading step k, the algorithm is the following one:

1. apply elastic loading $\mathbf{f}^{el}$,
2. compute $\mathbf{u}^{el}$ by solving the equilibrium equation,
3. compute $\theta_{\min}$ with
$$\theta_{\min} = \min_{\substack{i,j\in(1,..,n)\\ i\neq j}} \left(\frac{1}{P_{ij}}\right)$$
4. save couple $(\theta_{\min}\mathbf{u}^{el}, \theta_{\min}\mathbf{f}^{el})$,
5. change the stiffness matrix setting
$$\mathbf{K}^{k+1} = \mathbf{K}^{k} - \mathbf{L}_{ij}^{T}\mathbf{K}_{ij}\mathbf{L}_{ij}$$
where $\mathbf{L}_{ij}$ is the connectivity matrix of element ij.

A more classical algorithm with an incremental loading in displacement can obviously be used, but the uniqueness of the solution is not guaranteed especially for two large loading steps. Furthermore, snapback behavior occurring frequently for brittle material can not be reproduced with a increasing incremental loading.

3 REINFORCEMENT BARS

Including reinforcement bars in a discrete model can be done:

- by explicitly meshing the rebars (Shiu, Donzé, and Daudeville 2009),
- by introducing additional degrees of freedom (dof) for the rebars linked with the dofs of the initial random mesh through prescribed kinematic relations (Bolander and Saito 1998).

The drawbacks of these methods is the additional dofs and the nonlinear relations between dofs, that can lead to extra computer time to solve the problem. We propose here an efficient approach, from a numerical point of view, to include the rebars: no additional dofs are considered, and the initial elastic prediction algorithm, at least for an elastic behavior of the rebars, can still be used. The chosen strategy is then based on the following points:

- the reinforcement bars are modeled with Euler-Bernoulli beams, with suitable coefficients,
- the initial random Voronoi tessellation is locally aligned in order to follow the reinforced bars geometry.

3.1 *Rebars meshing*

The meshing steps are shown on figure 2 in a 2D case for a better visualization. The random Voronoi tessellation is obtained following the protocol presented in section 2.1. Then, all nuclei of particles crossed by a rebar are moved on the rebar line, and the new tessellation is computed (these different steps are strictly identical in 3D). A potential drawback of the method is that the mesh randomness, provided the isotropic properties of the medium, is lost around the bars (see the modification of the mesh on the bottom view in figure 2). This is not a real problem because the isotropic properties of a real reinforced concrete is obviously not verified around the rebars.

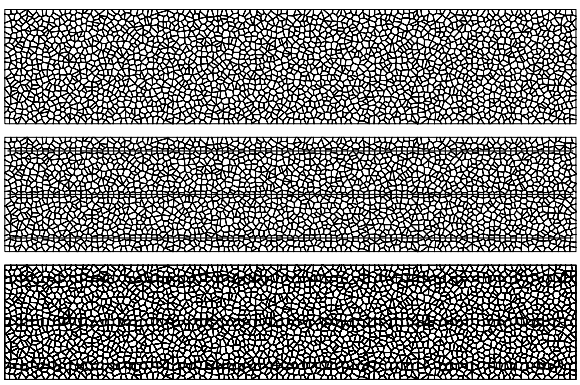

Figure 2. The initial mesh without rebars (top), the modified mesh with the rebars (middle), superposition of the initial and modified meshes (bottom).

The effect of the remeshing at the macroscale is studied on a 2D (table 1) and a 3D (table 2) samples, for different rebars arrangement (only the mesh is different, the beam parameters are unchanged in this part). The elastic modulus and the Poisson coefficient are given for the different configurations and compared to the initial random mesh. The variation of the global coefficient is less than 1% in both 2D and 3D cases, and is of order of the variation due to the mesh heterogeneity.

				
E_x (GPa)	32.0	32.1	32.2	32.1
E_y (GPa)	31.7	31.8	31.9	31.8
ν_x	.206	.205	.202	.205
ν_y	.206	.205	.202	.205

Table 1. 2D 128×128-particle samples (reference mesh, 2 horizontal rebars, 4 horizontal rebars, 2 vertical rebars). Model parameters are $E_b = 40$ GPa, $\alpha = 0.85$.

				
E_x (GPa)	29.9	29.8	30.1	29.9
E_y (GPa)	29.8	29.8	30.0	29.9
E_z (GPa)	29.9	29.9	30.0	30.1
ν_x	.203	.203	.201	.202
ν_y	.202	.203	.202	.202
ν_z	.203	.203	.202	.202

Table 2. 3D $20 \times 20 \times 20$-particle samples (reference mesh, 4 horizontal rebars, 9 horizontal rebars, 4 vertical rebars). Model parameters are $E_b = 48$ GPa, $\alpha = 0.77$.

3.2 *Rebars parameters*

Once the new mesh is obtained, the properties of the beams assigned to the rebars are changed. Two kinds of beams are considered. The first ones are the aligned beams representing the rebar, the second ones are the beams linking the rebars to concrete (figure 3).

The parameters of the rebar beams are easy to identify, especially in that case where an elastic behavior of the rebars is considered (ϕ is the rebar diameter):

- beam section: $A_b^s = \pi\phi^2/4$,
- beam inertia: $I_b^s = \pi\phi^4/64$,
- beam Young modulus: $E^s = 200$ MPa
- $\varepsilon_{ij}^{cr^s} = \theta_{ij}^{cr^s} = \infty$

The elastic parameters of the interface beams are equal to the elastic parameters of the beams used for plain material. The breaking parameter ε_{ij}^{cr} is also unchanged. Just the rotation breaking parameter θ_{ij}^{cr} is

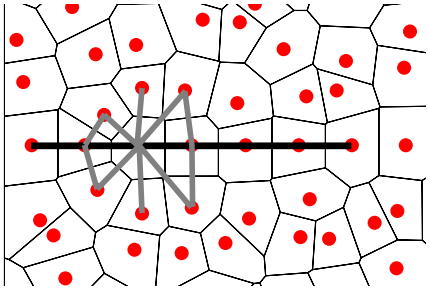

Figure 3. The two kinds of beams considered for the rebar: the black ones correspond to the rebar beams, the grey ones (just few of them are plotted on the figure) correspond to the interface beams.

changed, allowing to represent the decohesion of the steel with the concrete. We propose next to validate the model with results obtained from two experimental tests.

4 NUMERICAL APPLICATIONS

4.1 *Beam under tension*

The first validation test is the reinforced beam under tension proposed by (Mivelaz 2006). In this study, a 5m-length beam with a rectangular cross section of $1 \times .42$m has been tested. Different rebars arrangements and different concrete formulation have been considered in the study. We present here the results obtained with the AS5 reinforcement and a standard concrete (f_{c28}=39 MPa, f_{t28}=2.6 MPa, $E = 32$ GPa). The AS5 arrangement is composed of two lines of 12 ϕ16-rebars (figure 4).

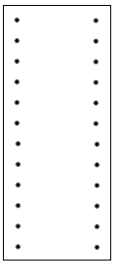

Figure 4. Beam cross section

The used mesh is shown on figure 5. It is composed of 3600 particles. The model parameters are $E_b = 47$ GPa, $\alpha = 0.74$, $\varepsilon_{cr} = 1.2e-4$, $\theta_{cr} = 8.0e-4$. The horizontal displacement on the left face and the displacements of point (0,0,0) are fixed. The loading is a uniform displacement applied on the right face.

The global force-strain evolution is presented on figure 6: after a first elastic evolution, a quasi-constant force is obtained, with different jumps corresponding to the apparition of macro-cracks perpendicular to the loading direction.

The cracking pattern is of main interest in this study, as an evaluation of the permeability of the cracked beam has been performed in the experimental study. We present in figure 7 three different cracking patterns obtained during the loading. The color scale represents the crack opening, evaluated with the displacement jump across the crack: for a crack separating particles i and j, the crack opening is computed as $e_{ij} = \langle(\mathbf{u}_j - \mathbf{u}_i).\mathbf{n_{ij}}\rangle$ where $\mathbf{u}_i$ and $\mathbf{u}_j$ are the displacement vectors of particles i and j. The notation $\langle x\rangle = \max(x, 0)$ is used for the positive part of a scalar. Note that for this homogeneous loading, the cracking pattern is different for each different mesh, due to the heterogeneity introduced in the model. The evolution of the opening of the first three cracks is presented on figure 8, with the evolution of opening of the first experimental crack. The numerical results show a very good agreement with the value obtained with the experimental test, in terms of evolution and magnitude.

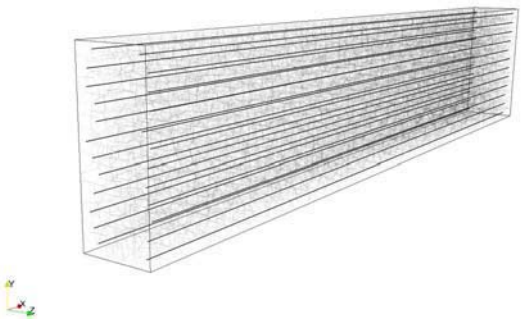

Figure 5. The discrete mesh of the Mivelaz beam.

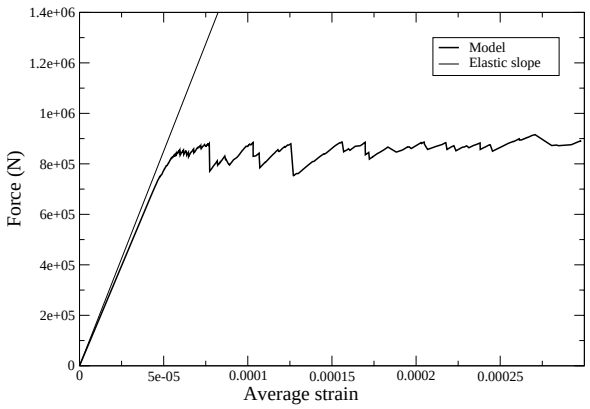

Figure 6. The force-strain curve.

4.2 *3-point bending test*

The next experimental test is a classical 3-point bending test on a reinforced concrete beam. The considered beam, with a length of 5m and a cross section of 0.2×0.5 m, is reinforced with $2\phi32$ bars in the lower part and $2\phi8$ bars in the upper part (figure 9). The first results were proposed by (Pera 1973) and have been analyzed in the "MECA" benchmark (Ghavamian, Carol, and Delaplace 2003). A second experimental campaign on the same beam has been recently proposed by (Grondin 2008). The beam has been tested until failure, and the apparition of cracking has been observed during the loading.

The used mesh is composed of $150 \times 15 \times 6$ par-

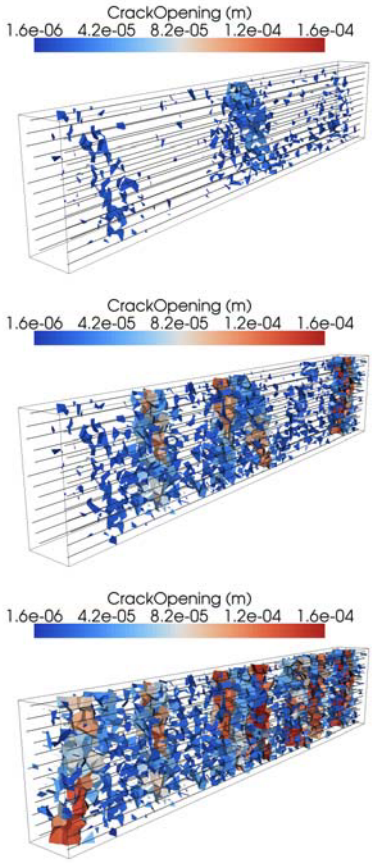

Figure 7. Cracking pattern of the Mivelaz beam.

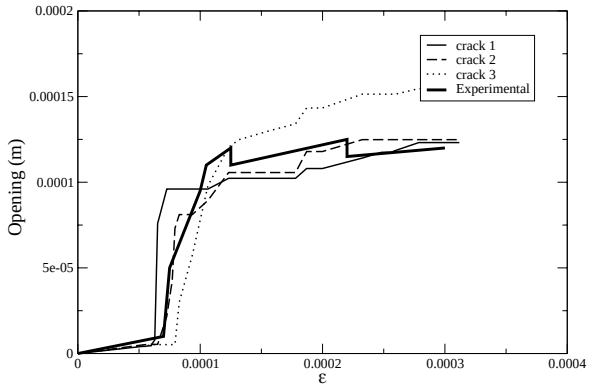

Figure 8. The opening measurement of the first three cracks, and the opening of the first experimental crack.

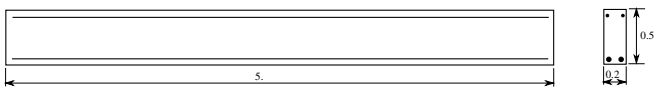

Figure 9. 3-point bending beam cross section (just the horizontal rebars are drawn).

ticles. For this first study, just the horizontal rebars have been modeled (figure 10). The model parameters are $E_b = 49.9$ GPa, $\alpha = 0.74$, $\varepsilon_{cr} = 1.24e-4$, $\theta_{cr} = 8.0e-4$.

The global reponse is plotted on figure 11. The classical evolution of a reinforced concrete beam is obtained, with a first elastic behavior followed by a stiffness decrease due to the damage of concrete. Note that for this loading, the rebars do not reach their plasticity limit: the failure of the beam is obtained for a lower force level because the stirrups are not considered in this computation.

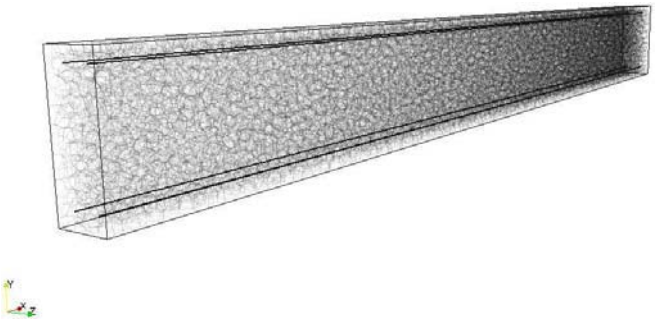

Figure 10. DEM mesh of the three-point-bending beam.

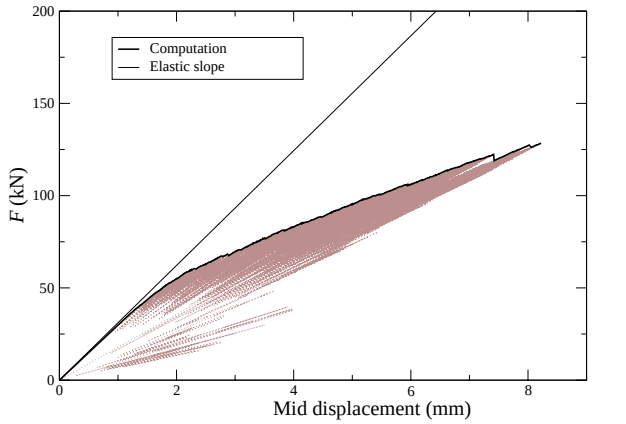

Figure 11. The evolution of the global force *vs* the mid-beam displacement.

The global cracking pattern is represented on figure 12. The first cracks initiate in the bottom of the beam and propagate to the central loading point on the upper face of the beam.

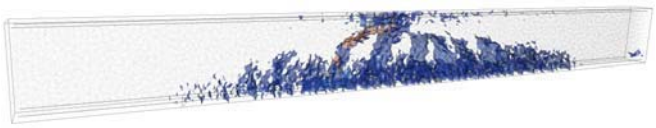

Figure 12. Cracked beam

As for the previous case, the evolution of the crack opening with the loading has been performed, although experimental data are not available. We limit the study to two cracks located in the central part of the beam, which propagate all along the loading. A cut of the numerical sample is shown of figure 13, with the two observed cracks surrounded by two rectangles. The evolution of their opening is plotted on figure 14.

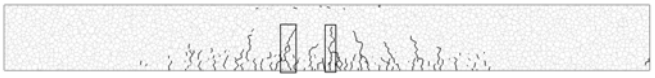

Figure 13. Slice of the cracked beam with the two observed cracks.

t

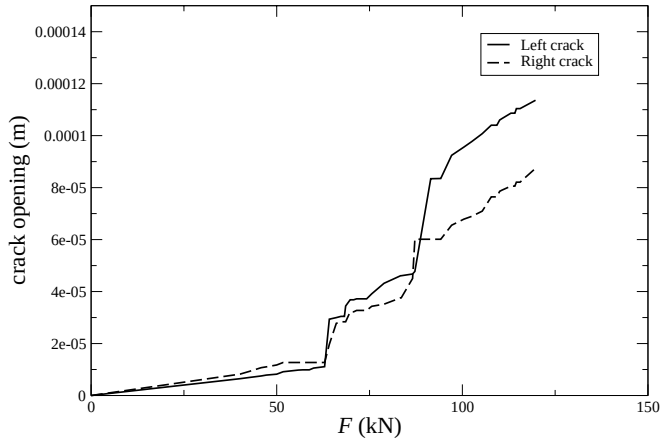

Figure 14. Evolution of the opening of two central cracks.

5 CONCLUSION

We propose in this study a non-intrusive procedure to take into account reinforcement bars in a discrete element model. The "non-intrusive" consideration means that the model basis is unchanged, the number of degrees of freedom is kept constant and more important the "elastic prediction" solver can still be used. This is an important point for ensuring the uniqueness of the numerical solution. The proposed approach is based on two steps:

- The first step consists in meshing the rebars by moving the nuclei of the Voronoi particles crossed by the rebars on the rebars lines. A numerical analysis shows that the effect of the local rearrangement can be neglected with respect to the variability of the response due to the mesh randomness.

- The second step consists in changing the local properties of the beam linking the rebars particles accounting for the steel material properties of the rebars.

The performance of the approach is shown on two experimental test, a simple tension test on a reinforced beam and a more classical three-point bending test. In both cases, the global force response is obtained. More interesting, a fine description of the cracking pattern is obtained, showing the capability of a discrete element approach to model cracking in brittle material. The evolution of the crack opening is also obtained and compared to the experimental values.

ACKNOWLEDGEMENTS: We thanks The French National Project CEOS.fr for financial support.

REFERENCES

Bolander, J. E. and S. Saito (1998). Fracture analysis using spring networks with random geometry. *Engineering Fracture Mechanics 61*, 569–591.

Chiaia, B., A. Vervuurt, and J. G. M. Van Mier (1997). Lattice model evaluation of progressive failure in disordered particle composites. *Eng. Fracture Mech. 57*(2/3), 301–318.

Cundall, P. A. and O. D. L. Strack (1979). A discrete numerical model for granular assemblies. *Géotechnique 29*, 47–65.

D'Addetta, G. A. (2004). *Discrete models for cohesive frictional materials*. Ph. D. thesis, Stuttgart University.

Delaplace, A. (2009). Tensile damage response from discrete element virtual testing. *Geomechanics and Geoengineering 4*(1), 79–89.

Delaplace, A. and R. Desmorat (2007). Discrete 3d model as complimentary numerical testing for anisotropic damage. *International Journal of Fracture 148*, 115–128.

Delaplace, A. and A. Ibrahimbegovic (2006). Performance of time-stepping schemes for discrete models in fracture dynamic analysis. *International Journal for Numerical Methods in Engineering 65*, 1527–1544.

Delaplace, A., S. Roux, and G. Pijaudier-Cabot (2001). Avalanche statistics of interface crack propagation in fiber bundle model: characterization of cohesive crack. *Journal of Engineering Mechanics 127*(7), 646–652.

Ghavamian, S., I. Carol, and A. Delaplace (2003). Discussion over meca project. *Revue Française de Génie Civil 7*(5), 543–581.

Grondin, P. (2008). Benchmark poutre flexion trois points. Technical report.

Herrmann, H. J. and S. Roux (1990). *Statistical models for the fracture of disordered media*. Elsevier Science Publishers, Amsterdam.

Kun, F. and H. Herrmann (1996). A study of fragmentation processes using a discrete element method. *Comp. Meth. Appl. Mech. Eng. 7*, 3–18.

Mivelaz, P. (2006). *Fuites au travers d'un lment fissur*. Ph. D. thesis, Ecole Polytechnique Fédérale de Lausanne.

Moukarzel, C. and H. J. Herrmann (1992). A vectorizable random lattice. *J. Stat. Phys. 68*, 911–923.

Pera, J. (1973). *Reinforced concrete redundant beams. Theoretical and experimental analysis*. Ph. D. thesis, INSA Lyon.

Rojek, J. and E. Onate (2007). Multiscale analysis using a coupled discrete/finite element model. *Interaction and Multiscale Mechanics 1*(1), 1–31.

Rots, J. G., S. Invernizzi, and B. Belletti (2006). Saw-tooth softening/stiffening - a stable computational procedure for rc structures. *Computers & Concrete 3*, 213–233.

Schlangen, E. and E. J. Garboczi (1997). Fracture simulations of concrete using lattice models: Computational aspects. *Eng. Fracture Mech. 57*(2/3), 319–332.

Shiu, W., F. Donzé, and L. Daudeville (2009). Discrete element modelling of missile impacts on a reinforced concrete target. *International Journal of Computer Applications in Technology 34*, 33–41.

Van Mier, J. G. M. and M. R. A. Van Vliet (2003). Influence of microstructure of concrete on size/scale effects in tensile fracture. *Engineering Fracture Mechanics 70*, 2281–2306.

Woestyn, S., A. Delaplace, and P. Koechlin (2006). Analyse de la rupture dynamique du béton par un modèle discret. *Revue Européenne de Génie Civil 10*, 1281–1308.

Xiao, S. and T. Belytschko (2004). A bridging domain decomposition for coupling continua with molecular dynamics. *Comput. Methods Appl. Mech. Engng. 193*, 1645–1669.